J. Fluid Mech. (1997), *vol.* 336, *pp.* 51–68

Copyright © 1997 Cambridge University Press

On the crest instabilities of steep surface waves

By MICHAEL LONGUET-HIGGINS[1] AND MITSUHIRO TANAKA[2]

[1] Institute of Nonlinear Science, University of California, San Diego, La Jolla, CA 92093-0402, USA

[2] Department of Applied Mathematics, Faculty of Engineering, Gifu University, 1-1 Yanagido, Gifu 501-11, Japan

(Received 19 April 1996 and in revised form 28 August 1996)

The forms of the superharmonic instabilities of irrotational surface waves on deep water are calculated for wave steepnesses up to 99.9 % of the limiting value. It is found that as the limiting wave steepness is approached the rates of growth of the lowest two unstable modes ($n = 1$ and 2) increase according to the asymptotic law suggested by the theory of the almost-highest wave (Longuet-Higgins & Cleaver 1994; Longuet-Higgins, Cleaver & Fox 1994; Longuet-Higgins & Dommermuth 1997). Moreover, each eigenfunction becomes concentrated near the wave crest, with a horizontal scale proportional to the local radius of curvature at the crest. These are therefore 'crest instabilities' in the original sense.

Similar calculations are carried out for the normal-mode instabilities of solitary waves in shallow water, at steepnesses up to 99.99 % of the limiting steepness. Similar conclusions are found to apply, though with greater accuracy.

1. Introduction

The stability of a train of steep, progressive, irrotational waves in water of finite or infinite depth is of some interest in connection with the theory of wave breaking. Subharmonic instabilities, having wavelengths larger than the basic wavelength $2\pi/k$, can occur at relatively low wave steepness. But if we confine attention to the superharmonic instabilities, that is to say two-dimensional instabilities having the same space-periodicity as the unperturbed wave, then it is found that only very steep gravity waves are appreciably unstable.† In deep water it was shown numerically by Tanaka (1983) and analytically by Saffman (1985) that gravity waves first become unstable in this way when the steepness parameter ak attains the value 0.4292, corresponding to the first maximum in the total energy density. Similarly, for solitary waves Tanaka (1986) showed that instability first occurred at a height-to-depth ratio $a/h = 0.7824$, which again corresponded to the first maximum in the total wave energy E.

The wave steepnesses just mentioned are already high, being close to the limiting steepnesses: $ak = 0.4432$ for a wave in deep water and $a/h = 0.8332$ for the solitary wave. Calculation of the properties of such steep waves by ordinary methods presents increasing difficulties as the limiting wave is approached. It was therefore of some interest when Longuet-Higgins & Fox (1977) showed that the crest of any steep Stokes wave (not the steepest) approached a certain asymptotic form characterized by a length scale

$$l = q^2/2g, \tag{1.1}$$

† We are excluding the 'bubbles' of non-stationary instability pointed out by MacKay & Saffman (1986) and Kharif & Ramamonjiarisoa (1990).

https://doi.org/10.1017/S0022112096004028 Published online by Cambridge University Press

where q is the particle velocity at the wave crest in a reference frame moving with the phase speed c, and g denotes gravity. The flow has a rounded crest at the origin, and at infinity tends to the well-known 120° corner flow. In a second paper Longuet-Higgins & Fox (1978) showed how to fit this inner flow to the outer flow in a wave in deep water by an asymptotic matching technique assuming the parameter

$$\epsilon^2 = gl/c_0^2 \tag{1.2}$$

to be small, $c_0 = (g/k)^{1/2}$ being the linear phase speed. A corresponding theory for solitary waves, in which $c_0 = (gd)^{1/2}$, has been given by Longuet-Higgins & Fox (1996).

Now in two recent papers (Longuet-Higgins & Cleaver 1994; Longuet-Higgins, Cleaver & Fox 1994) it was suggested that for very steep waves the lowest superharmonic instability of a progressive wave should correspond, in the limit as $\epsilon \to 0$, with an instability of the *inner* flow of the almost-highest wave. The lowest instability of the inner flow was therefore calculated, also the first-order correction to this instability resulting from the matching process. The growth rates of the instability apparently agreed with those found numerically by Tanaka (1983) for progressive waves of finite amplitude. Tanaka's calculations, however, at that time extended only as far as $ak = 0.439$, and no eigenfunctions were available. One of us (M.S.L.-H.) therefore proposed to Tanaka to extend his calculations (with a more modern computer) to higher values of ak and to calculate if possible the corresponding eigenfunctions. It is these calculations, first presented last year (Tanaka 1995), that are reported fully in the present paper. We report also similar calculations for solitary waves which are more accurate than those for periodic waves.

The calculations by Tanaka (1995) showed the need for a re-examination of the numerical calculation reported in Longuet-Higgins & Cleaver (1994) and Longuet-Higgins *et al.* (1994). This has led to a significant improvement in their accuracy (see Longuet-Higgins & Dommermuth 1997, referred to herein as LHD). As will be shown here, the revised values of the rate of growth as $\epsilon \to 0$ agree satisfactorily with those reported by Tanaka (1995), especially for the lowest mode ($n = 1$). The revised calculations also show the presence of a second mode ($n = 2$) as was originally suggested by Cleaver (1981); this also is consistent with Tanaka's (1995) calculations.

The plan of this paper is as follows. In §§2 and 3 we describe the method of computation, and the numerical results, for steep periodic waves in deep water, and in §§4 and 5 we present corresponding results for the solitary wave in shallow water. In §6 we compare the two sets of results with one another and with the eigenfunctions obtained by LHD for the limiting case $\epsilon \to 0$. A discussion follows in §7.

2. Numerical results for Stokes waves in deep water

To calculate the flow in a steady, irrotational gravity wave of finite amplitude in deep water we have used the method described in Tanaka (1983). Waves of a given amplitude are distinguished by a parameter $\omega = 1 - q_c/q_t$, where q_c and q_t are the particle speed at the crest and the trough, respectively, observed in a reference frame moving with the Stokes wave. The parameter ω is more suitable as the amplitude parameter than ak in the sense that its range is known *a priori* to be $0 \leqslant \omega \leqslant 1$. Thus $\omega = 0$ corresponds to the wave with infinitesimal amplitude, while $\omega = 1$ corresponds to the limiting wave with a stagnation point at its crest (i.e. $q_c = 0$). The range of ω that we treat here is $0.80 \leqslant \omega \leqslant 0.97$. (Note that ω behaves similarly to the parameter ω' used by Longuet-Higgins & Fox 1978.)

https://doi.org/10.1017/S0022112096004028 Published online by Cambridge University Press

	N	ak	c	error (%)
$\omega = 0.80$	64	0.426736789	1.091569934 8	1.805×10^{-4}
	128	0.426736861 9	1.091569935 0	3.820×10^{-10}
	256	0.426736861 9	1.091569935 0	1.602×10^{-10}
$\omega = 0.97$	512	0.442616671 5	1.092269082 2	5.260×10^{0}
	1024	0.442754143 6	1.092276960 4	5.666×10^{-3}
	2048	0.442754222 4	1.092276960 4	1.258×10^{-8}

TABLE 1. Convergence of the Stokes wave in deep water

ω	ak	ϵ	c/c_0	Rk/ϵ^2
0.80	0.426 74	0.188 58	1.091 57	5.3274
0.81	0.428 55	0.179 17	1.092 01	5.3063
0.82	0.430 22	0.169 74	1.092 35	5.2869
0.83	0.431 73	0.160 30	1.092 61	5.2692
0.84	0.433 12	0.150 86	1.092 79	5.2529
0.85	0.434 37	0.141 41	1.092 90	5.2382
0.86	0.435 51	0.131 96	1.092 95	5.2248
0.87	0.436 55	0.122 51	1.092 94	5.2128
0.88	0.437 49	0.113 07	1.092 89	5.2021
0.89	0.438 35	0.103 62	1.092 82	5.1926
0.90	0.439 12	0.094 19	1.092 72	5.1843
0.91	0.439 83	0.084 75	1.092 61	5.1772
0.92	0.440 47	0.075 33	1.092 51	5.1711
0.93	0.441 06	0.065 91	1.092 42	5.1659
0.94	0.441 58	0.056 49	1.092 35	5.1618
0.95	0.442 04	0.047 07	1.092 31	5.1585
0.96	0.442 44	0.037 66	1.092 28	5.1560

TABLE 2. Calculated values of the parameters for periodic waves in deep water

Table 1 shows the convergence of the steepness parameter ak and the phase speed c as the number N of Fourier modes used to express the flow is increased, for the cases $\omega = 0.80$ and $\omega = 0.97$. The maximum deviation of the Bernoulli constant $\frac{1}{2}q^2 + gy$ along the free surface is also shown. The limiting value of ak is known to be 0.4432, hence the ak of the two cases shown in the table are about 96.3 % and 99.9 % of the limiting value. The table shows that $N = 128$ is sufficient to get the convergence of c to the ten decimal places for $\omega = 0.80$, while more than $N = 1024$ is necessary to get the same convergence when $\omega = 0.97$. The speed of convergence of the series representing the Stokes wave also determines the speed of convergence of the solution of the eigenvalue problem in the stability analysis, and this rapid slowdown of convergence for larger values of ω causes serious difficulty in the stability calculation later.

The range $0.80 \leqslant \omega \leqslant 0.97$ corresponds to $0.1886 \geqslant \epsilon \geqslant 0.0282$, see table 2. Within this range of ϵ the asymptotic relations for ak and c derived by Longuet-Higgins & Fox (1978) coincide with our numerical results up to four significant figures. The last column of table 2 shows the radius of curvature R at the crest converging to the value $5.15\epsilon^2$ predicted in Longuet-Higgins & Fox (1977). According to the asymptotic theory for the deep-water wave given in Longuet-Higgins & Fox (1978), the lowest-

https://doi.org/10.1017/S0022112096004028 Published online by Cambridge University Press

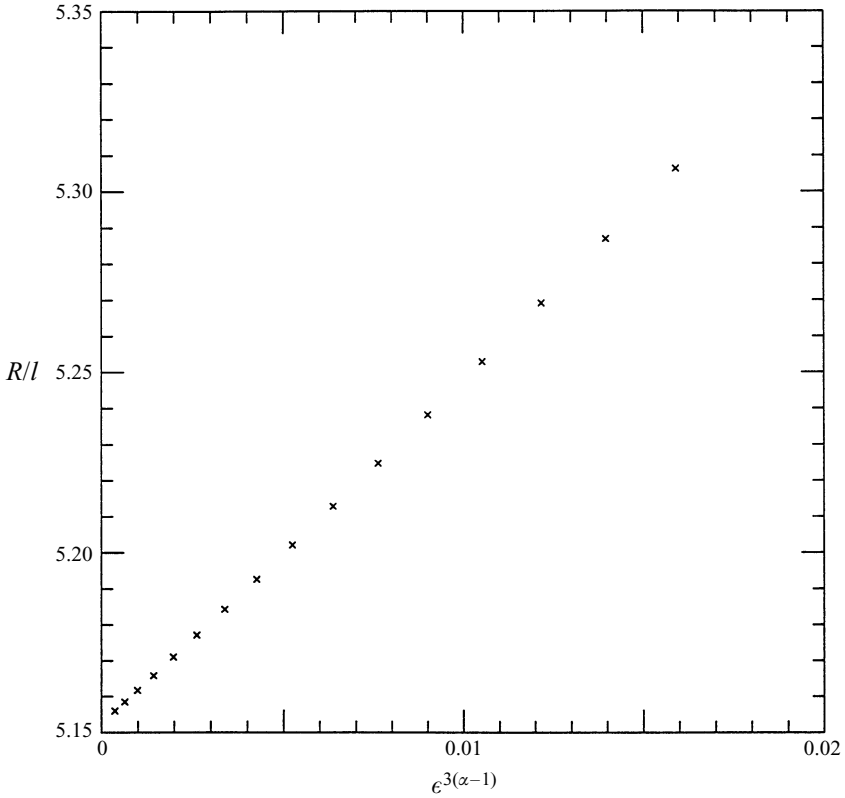


FIGURE 1. The scaled crest curvature R/l for deep-water waves, as a function of $\epsilon^{3(\alpha-1)}$.

order correction to the inner solution is proportional to $\epsilon^{3(\alpha-1)}$ where α is the lowest root of the transcendental equation

$$\tfrac{1}{2}\pi\alpha \tan \tfrac{1}{2}\pi\alpha = -\frac{\pi}{2\sqrt{3}}, \tag{2.1}$$

that is to say $\alpha = 1.8027$. In figure 1 we have plotted R/l against $\epsilon^{3(\alpha-1)}$, that is $\epsilon^{2.4081}$ and it can be seen that the plots lie almost on a straight line. (A small oscillation about this line is also to be expected from the analysis.) From figure 1 we may deduce the more accurate expression

$$R/l \simeq 5.1525 + 9.5\,\epsilon^{3(\alpha-1)} \tag{2.2}$$

for the crest curvature R.

3. Normal modes of instability

In this Section we consider the normal modes of perturbation of the steady waves calculated in §2, that is to say we seek those small perturbations whose time-dependence is like $e^{\lambda t}$, where λ is a constant. The numerical method whereby the problem is reduced to finding the eigenvalues and eigenfunctions of a pure imaginary square matrix is explained in detail in Tanaka (1983). As mentioned in §1, for low values of the wave steepness ak, or equivalently for low values of ω all the eigenvalues λ_n are pure imaginary and the normal modes behave sinusoidally in time. At comparatively large values of ak or ω, there appear one or more real eigenvalues, each corresponding to a perturbation which either grows or decays exponentially with t.

https://doi.org/10.1017/S0022112096004028 Published online by Cambridge University Press

	N_e	λ_1^2		N_e	λ_1^2
$\omega = 0.80$	10	−0.022 76	$\omega = 0.97$	70	2.947 71
	15	−0.018 20		120	2.632 95
	20	−0.015 06		200	2.451 13
	30	−0.014 88		300	2.404 13
	50	−0.014 88		400	2.397 50
	70	−0.014 88		500	2.396 59

TABLE 3. Convergence of the eigenvalue of the lowest mode

ω	E	λ_1^2	$(\epsilon\lambda_1)^2$	λ_2^2	$(\epsilon\lambda_2)^2$
0.80	0.073 991	−0.014 88	−0.000 529	−0.537 23	−0.019 105
0.81	0.074 032	−0.003 99	−0.000 128	−0.508 17	−0.016 312
0.82	0.074 026	0.007 66	0.000 221	−0.478 64	−0.013 790
0.83	0.073 979	0.020 26	0.000 521	−0.448 60	−0.011 528
0.84	0.073 898	0.034 11	0.000 776	−0.418 00	−0.009 513
0.85	0.073 791	0.049 57	0.000 991	−0.386 75	−0.007 734
0.86	0.073 668	0.067 18	0.001 170	−0.354 80	−0.006 178
0.87	0.073 534	0.087 74	0.001 317	−0.322 06	−0.004 834
0.88	0.073 399	0.112 38	0.001 437	−0.288 49	−0.003 688
0.89	0.073 268	0.142 88	0.001 534	−0.254 06	−0.002 728
0.90	0.073 149	0.181 97	0.001 614	−0.218 83	−0.001 941
0.91	0.073 046	0.234 05	0.001 681	−0.182 94	−0.001 314
0.92	0.072 964	0.306 43	0.001 739	−0.146 57	−0.000 832
0.93	0.072 904	0.411 79	0.001 789	−0.109 81	−0.000 477
0.94	0.072 867	0.573 90	0.001 831	−0.072 19	−0.000 230
0.95	0.072 849	0.842 16	0.001 866	−0.031 97	−0.000 071
0.96	0.072 847	1.334 68	0.001 893	0.015 93	0.000 023
0.97	0.072 852	2.396 59	0.001 912	0.087 42	0.000 070

TABLE 4. Calculated values of the total energy density E and of the squared eigenfrequencies of the normal-mode perturbations of a deep-water wave

Table 3 shows the convergence of the square of the eigenvalue λ_1 of the mode $n = 1$ for the deep-water waves with $\omega = 0.80$ and $\omega = 0.97$. In these tables, N_e is the number of Fourier modes which are used to express the eigenfunctions and does not have any direct relation with N of table 1 besides the trivial relation $N_e < N$. In terms of N_e the size of the matrix whose eigenvalue problem we need to solve is $(2N_e+1)\times(2N_e+1)$. When $\omega = 0.80$ we can have convergence of λ_1^2 to five decimal places with $N_e = 30$, while for $\omega = 0.97$ we get the convergence to only two decimal places even when N_e is increased to 400. When $\omega = 0.97$ and $N_e = 400$, the total CPU time used in the construction of the matrix and the calculation of all the eigenvalues and the eigenvectors was about 12 s on VP2600 of the Computation Center of Nagoya University.

In the analysis of the local flow around the crest by LHD time and space are normalized in such a way that $g = 1$ and $q_c = \sqrt{2}$, while in our calculations they are normalized such that $g = k = 1$ for the Stokes waves in deep water. The propagation speed of the basic steady wave c_0 in the limit of infinitesimal amplitude equals 1. In order to compare our results with those of LHD, we need to multiply our quantities by ϵ^{-2} for each dimension of space and ϵ^{-1} for each dimension of time.

https://doi.org/10.1017/S0022112096004028 Published online by Cambridge University Press

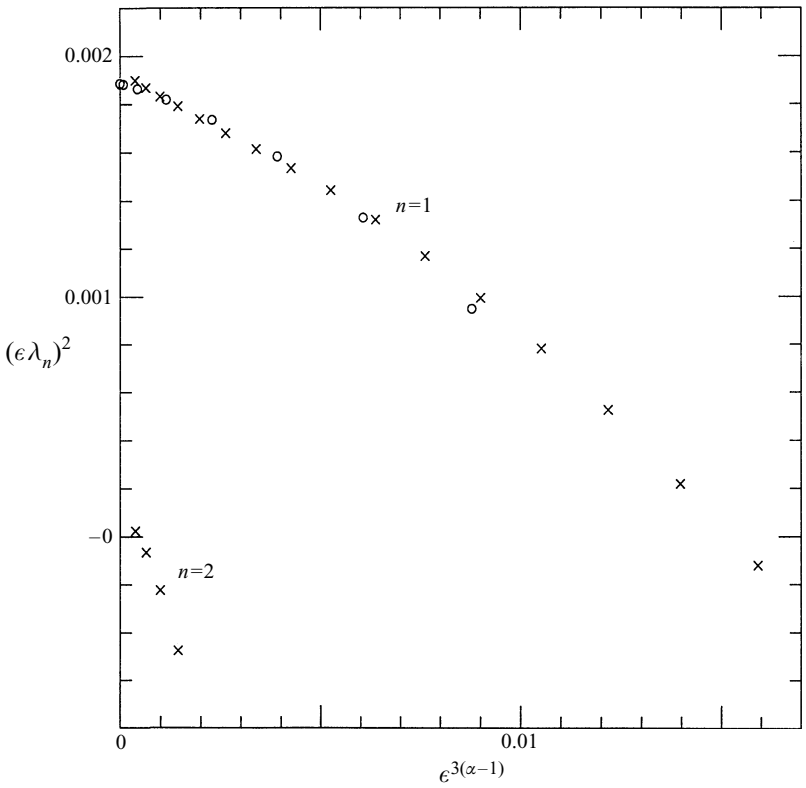


FIGURE 2. Squares of the growth rates λ_n of the two lowest modes of instability of the deep-water wave, scaled by the parameter ϵ, shown as a function of $\epsilon^{3(\alpha-1)}$. Crosses denote present calculation; circles, the asymptotic theory of the almost-highest wave, from Longuet-Higgins & Dommermuth (1997).

The square of the scaled eigenvalues $\epsilon\lambda_1$ $\epsilon\lambda_2$ of the two lowest eigenmodes $n = 1$ and $n = 2$ are shown in table 4 and plotted in figure 2. The time-dependence of the perturbation is assumed here to be like $e^{\lambda t}$, hence $\lambda^2 > 0$ implies instability. On the other hand the asymptotic theory given in Longuet-Higgins *et al.* (1994) and LHD indicates that the lowest-order corrections to the eigenfrequencies of the inner flow vary as $\epsilon^{3(\alpha-1)}$. In figure 2 we therefore plot the results as functions of $\epsilon^{3(\alpha-1)}$. As expected we see that the plots indeed fall approximately on a straight line, for small ϵ. A slight oscillation about the straight line is also seen.

Figure 2 also shows the corresponding results from LHD, and it will be seen there is close agreement over the expected range of ϵ.

Figure 3 shows the profile of the lowest unstable mode ($n = 1$) as a function of the horizontal coordinate x for $\omega = 0.84$, 0.88 and 0.92. It can be seen that as ω increases the perturbation progressively shrinks and is confined to a narrower region around the crest (which is at $x = 0$). The arrow in the figure indicates the direction of propagation of the Stokes wave. The amplitude of the normal mode, which is arbitrary within the framework of the linear stability analysis, is normalized in such a way that the maximum deviation of the profile is equal to unity, and this convention will be used throughout this paper.

Figure 4 shows the profiles of the same normal mode as those shown in figure 3, but as functions of the scaled horizontal coordinate x/ϵ^2. The widths of the curves are now

https://doi.org/10.1017/S0022112096004028 Published online by Cambridge University Press

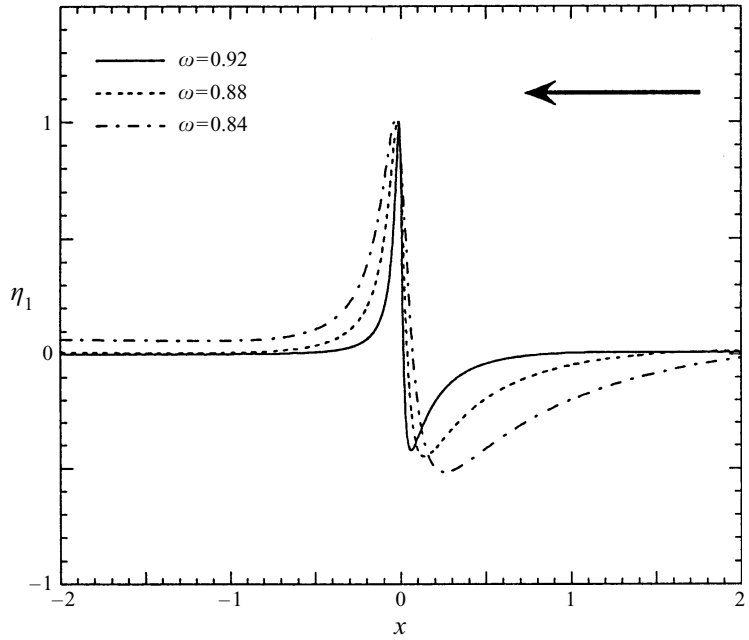


FIGURE 3. Vertical displacement η_1 in the lowest unstable mode of a deep-water wave as a function of the horizontal coordinate x, when $\omega = 0.84$, 0.88 and 0.92.

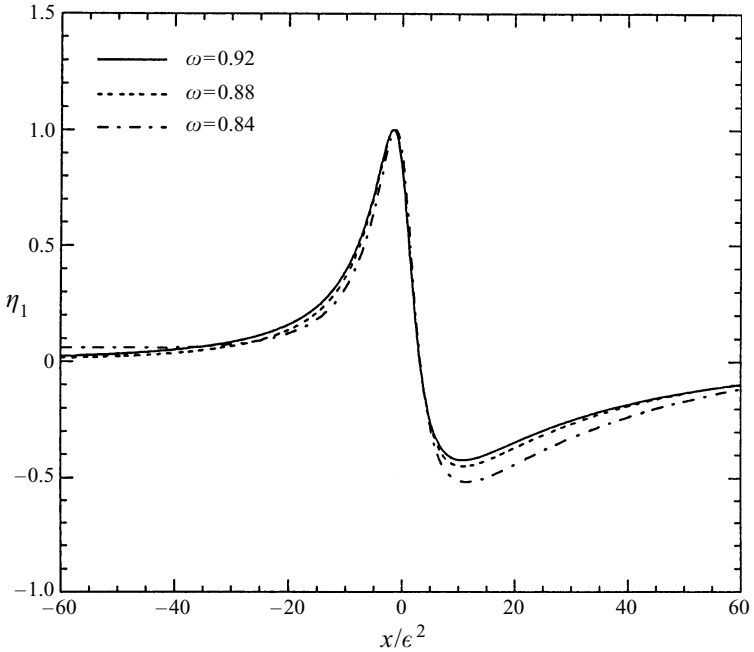


FIGURE 4. Vertical displacement η_1 in the lowest unstable mode of a deep-water wave as a function of the scaled coordinate x/ϵ^2, when $\omega = 0.84$, 0.88 and 0.92.

https://doi.org/10.1017/S0022112096004028 Published online by Cambridge University Press

comparable, but the values of ω do not seem to be large enough for a discussion of the asymptotic behaviour as $\epsilon \to 0$. Nevertheless we can clearly observe a tendency to converge towards some specific profile as $\omega \to 1$ ($\epsilon \to 0$).

The second mode $n = 2$ has just become unstable for the steepest case $\omega = 0.97$, and it seems obvious that we need to carry on to larger values of ω in order to discuss the asymptotic behaviour of the normal modes. For the case of $\omega = 0.97$, we need to solve the eigenvalue problem of a matrix larger than 800×800 in order to obtain the convergence of λ_2^2 to three significant figures as we mentioned before. Although the calculation for steeper cases is simple and straightforward, we did not carry it out for reasons of expense. As we shall see, greater accuracy is attainable in the case of solitary wave perturbations.

4. Numerical results for solitary waves in shallow water

The method which we employ here for calculating steady solitary waves is the same as that explained in detail in Tanaka (1986). In this method, steady solitary waves with different wave heights are distinguished by a parameter q/c where $q = q_c$, the particle velocity at the wave crest. In common with ω used for the deep-water waves in the previous section, the range of q/c is known *a priori* to be $0 \leqslant q/c \leqslant 1$. Unlike ω, however, q/c decreases as the wave gets steeper: $q/c = 1$ corresponds to the solitary wave with infinitesimal wave height, while $q/c = 0$ corresponds to the limiting solitary wave characterized by a 120° angular corner with a stagnation point ($q = 0$) at the crest. The range of q/c we treat here is $0.01 \leqslant q/c \leqslant 0.30$. Values of the wave height H and phase speed c at given values of q/c are shown in table 5; also shown is the radius of curvature R at the wave crest. As in §§2 and 3 we may define an inner length scale $l = q^2/2g$ and a small parameter

$$\epsilon'^2 = gl/c_0^2, \quad c_0^2 = gd, \tag{4.1}$$

which tends to zero as the wave approaches its limiting steepness, but since the value of c_0^2 here differs from the deep-water case the corresponding value of ϵ' is not precisely equivalent to the ϵ of §§2 and 3 and so will be distinguished with a prime.

Unlike the deep-water wave in which we employed spectral representation for both the deep-water wave and the perturbations to it, we use for the solitary wave a more direct method in which the basic solitary wave and the perturbations are both represented by the values at a discrete set of M points properly distributed along the free surface. In our calculations a solitary wave and the perturbations to it are always calculated at the same set of points.

Table 6 shows the convergence of the phase speed c, the wave height H and the square of the eigenvalues λ_1 and λ_2 of the two lowest unstable modes, in the case $q/c = 0.01$, as the number of nodes is increased.

Under the normalization $g = 1$ and $d = 1$, the limiting height for the steady solitary wave H_{max} is known to be 0.833 22, hence the wave height of the highest solitary wave shown in table 5 is about 99.99 % of H_{max}. For the steepest deep-water wave that was treated in the previous section q/c was about 0.05, so it can be said that the solitary wave shown in table 6 is much closer to the limiting wave than the steepest deep-water wave that we treated. Table 6 shows that even for such a steep solitary wave, we can obtain convergence up to nine significant figures for c and up to four significant figures for λ_1^2 with $M = 60$ only. The size of the matrix whose eigenvalue problem needs to be solved in the stability analysis of the solitary wave is $(2M-1) \times (2M-1)$. This much faster convergence suggests that the solitary wave case should be much more promising

https://doi.org/10.1017/S0022112096004028 Published online by Cambridge University Press

q/c	H/d	ϵ'	c/c_0	$R/\epsilon'^2 d$
0.01	0.833 12	0.009 13	1.290 89	5.152 64
0.02	0.832 86	0.018 26	1.290 89	5.153 34
0.03	0.832 43	0.027 38	1.290 88	5.154 76
0.04	0.831 83	0.036 51	1.290 86	5.157 03
0.05	0.831 06	0.045 64	1.290 85	5.160 28
0.06	0.831 06	0.054 77	1.290 86	5.164 59
0.08	0.827 98	0.073 03	1.290 98	5.176 74
0.10	0.825 36	0.091 31	1.291 27	5.194 17
0.12	0.822 28	0.109 61	1.291 74	5.217 50
0.14	0.818 69	0.127 93	1.292 33	5.247 40
0.16	0.814 48	0.146 28	1.292 96	5.284 57
0.18	0.809 54	0.164 64	1.293 56	5.329 79
0.20	0.803 74	0.183 00	1.294 01	5.383 90
0.22	0.796 95	0.201 33	1.294 21	5.447 85
0.24	0.789 08	0.219 61	1.294 07	5.522 66
0.25	0.784 72	0.228 72	1.293 85	5.564 50
0.26	0.780 05	0.237 81	1.293 52	5.609 50
0.28	0.767 98	0.255 90	1.292 49	5.709 66
0.30	0.758 24	0.273 85	1.290 92	5.824 58

TABLE 5. Parameters for the solitary wave

M	$c/(gd)^{1/2}$	H/d	$(\lambda_1 d/c)^2$	$(\lambda_2 d/c)^2$
30	1.290 887 661 8	0.833 112 158 1	13.0763	0.682 318
40	1.290 890 671 2	0.833 116 042 6	13.9659	0.713 888
50	1.290 890 857 1	0.833 116 282 5	13.8925	0.714 442
60	1.290 890 882 3	0.833 116 315 0	13.8940	0.714 884
70	1.290 890 886 6	0.833 116 320 5	13.8931	0.714 946
80	1.290 890 887 4	0.833 116 321 6	13.8930	0.714 966
90	1.290 890 887 6	0.833 116 321 8	13.8929	0.714 973

TABLE 6. Convergence of the solitary wave and the eigenvalues of the two lowest eigenmodes when $q/c = 0.01$

than the deep-water wave case for our present purpose which is to clarify the asymptotic behaviour of unstable normal modes as $\epsilon \to 0$.

Table 5 indicates that the scaled radius of curvature R/l approaches the theoretical value 5.15 as before. According to the asymptotic theory for steep solitary waves (Longuet-Higgins & Fox 1996) we expect the lowest-order corrections to the inner solution to be of order $\epsilon'^{[3(\alpha-1)]}$, as for the deep-water wave. Accordingly in figure 5 we have plotted R/l against $\epsilon'^{[3(\alpha-1)]}$ and we obtain as previously an almost straight-line plot.

5. Eigenmodes for the solitary wave

As shown in figure 6, the total energy of the solitary wave exhibits three stationary values within the range $0.01 < q/c < 0.30$. This behaviour of E is in agreement with the known asymptotic theory for steep solitary waves (Longuet-Higgins & Fox 1996). Hence when $q/c = 0.01$ we expect the existence of three unstable normal modes.

https://doi.org/10.1017/S0022112096004028 Published online by Cambridge University Press

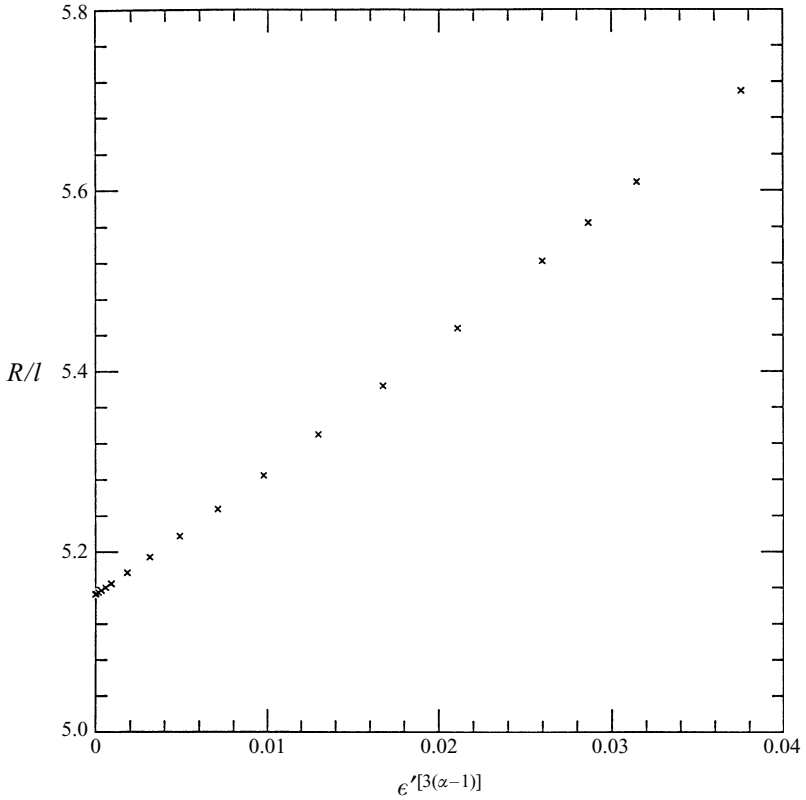


FIGURE 5. The scaled crest curvature R/l for solitary waves, as a function of $\epsilon'^{[3(\alpha-1)]}$.

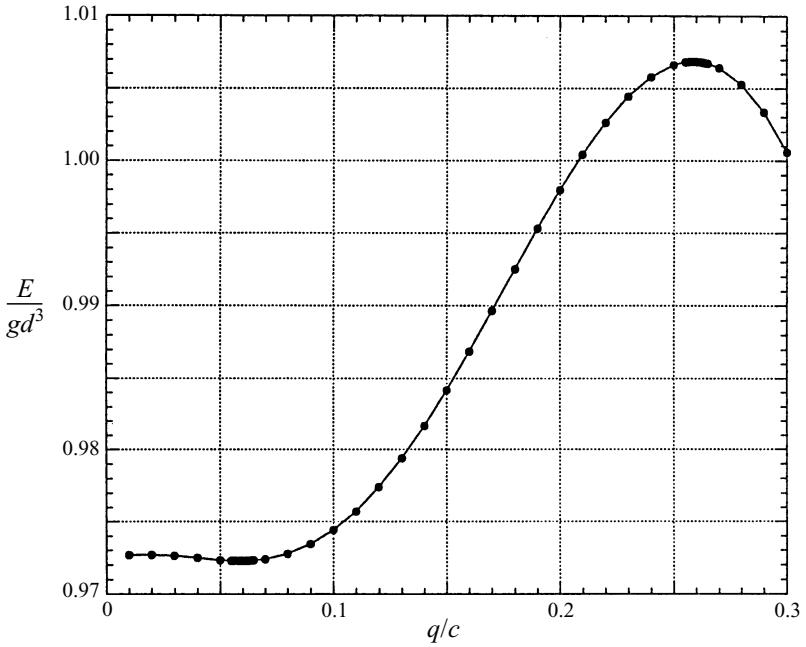


FIGURE 6. The total energy E of the solitary wave as a function of the parameter q/c.

https://doi.org/10.1017/S0022112096004028 Published online by Cambridge University Press

q/c	I	E	λ_1^2	λ_2^2
0.01	2.54347	0.97268	13.89290	0.71497
0.02	2.54347	0.97268	3.45947	0.15537
0.03	2.54337	0.97260	1.52518	0.05006
0.04	2.54315	0.97246	0.84689	0.01488
0.05	2.54286	0.97233	0.53209	0.00242
0.06	2.54261	0.97228	0.36050	
0.08	2.54275	0.97275	0.18886	
0.10	2.54449	0.97439	0.10866	
0.12	2.54839	0.97738	0.06489	
0.14	2.55467	0.98164	0.03875	
0.16	2.56312	0.98684	0.02242	
0.18	2.57325	0.99248	0.01211	
0.20	2.58438	0.99795	0.00577	
0.22	2.59567	1.00260	0.00215	
0.24	2.60620	1.00578	0.00043	
0.25	2.61089	1.00661	0.00008	
0.26	2.61506	1.00685		
0.28	2.62138	1.00527		
0.30	2.62436	1.00057		

TABLE 7. Calculated values of the impulse I and total energy E of the solitary wave, and of the squared growth rates of the two lowest instabilities

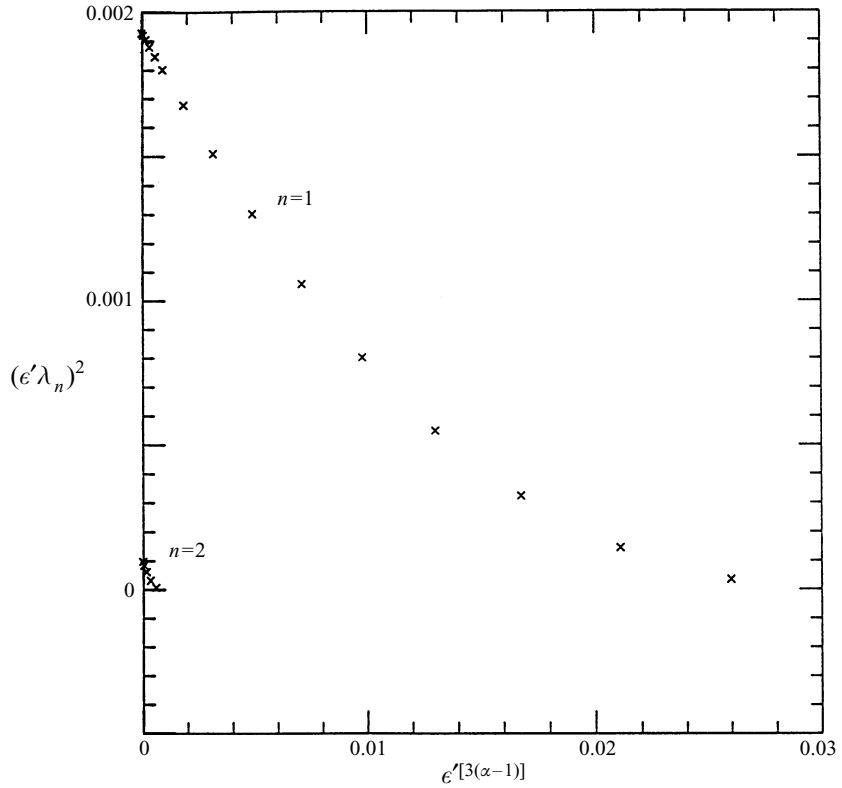


FIGURE 7. Scaled values of the squared growth rates of the two lowest modes of instability of the solitary wave, as a function of $\epsilon'^{[3(\alpha-1)]}$.

https://doi.org/10.1017/S0022112096004028 Published online by Cambridge University Press

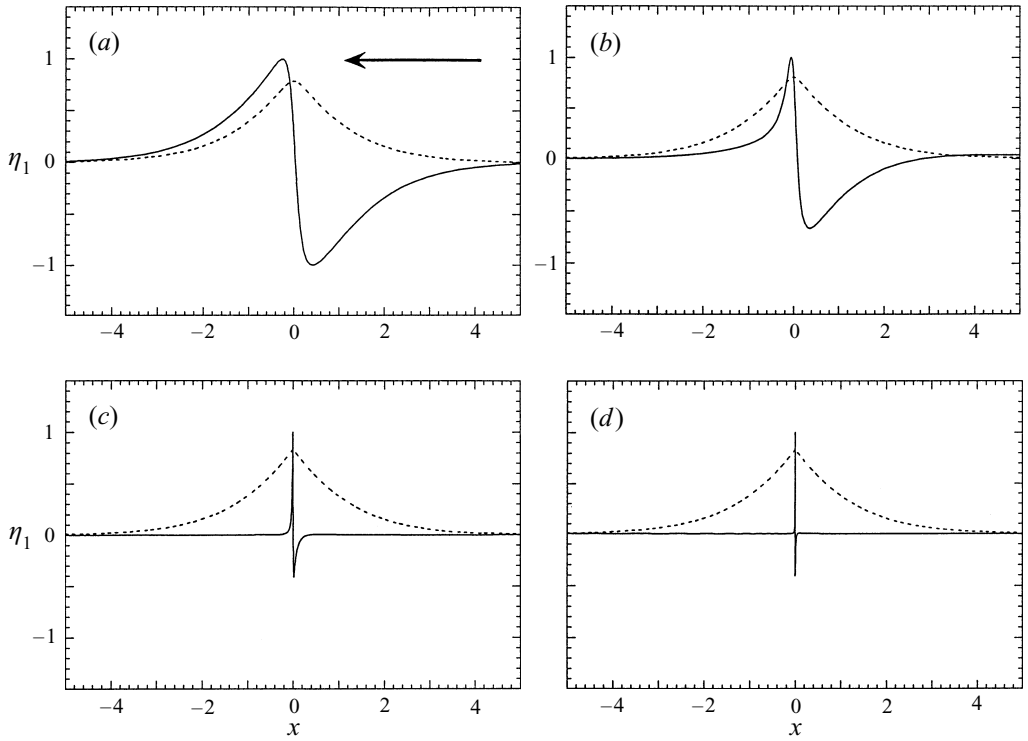


FIGURE 8. Profile of the first unstable mode of the solitary wave (solid line). The dashed curve shows the unperturbed wave profile: (*a*) $q/c = 0.25$, (*b*) $q/c = 0.20$, (*c*) $q/c = 0.10$, (*d*) $q/c = 0.02$.

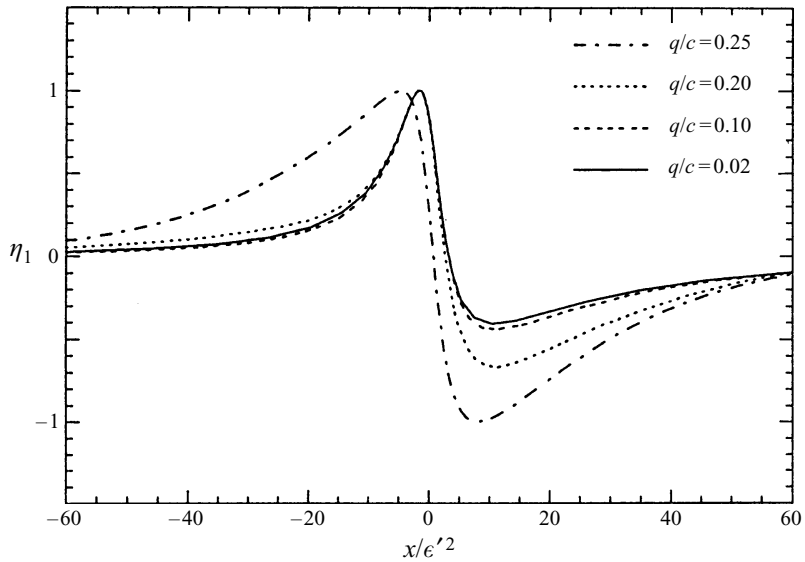


FIGURE 9. Profiles of the first unstable mode of the solitary wave plotted against the scaled coordinate x/ϵ'^2.

https://doi.org/10.1017/S0022112096004028 Published online by Cambridge University Press

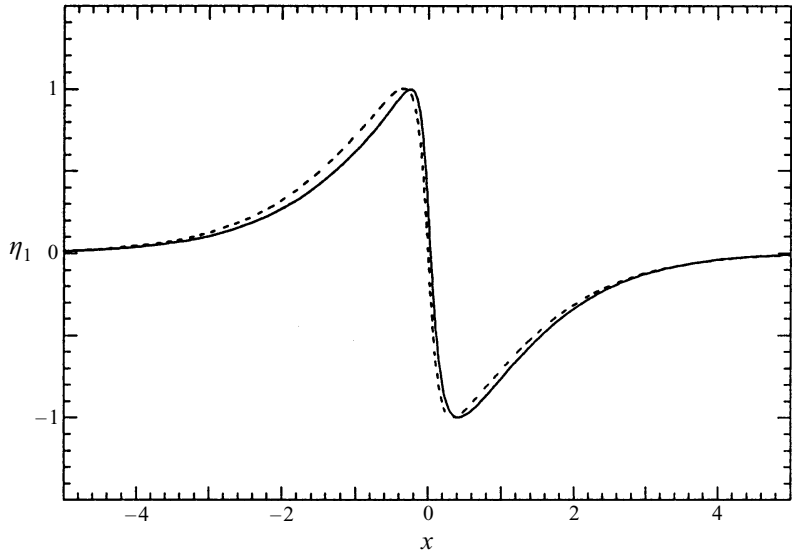


FIGURE 10. Comparison of the first unstable mode of the solitary wave when $q/c = 0.25$ (solid curve) with a pure phase shift (dashed curve).

Numerical values of the total impulse and energy are given in table 7, along with the squared growth rates of the two lowest instabilities.

In figure 7 we show the square of the scaled eigenvalues $\epsilon'\lambda_n$ of the two lowest unstable modes plotted as functions of $\epsilon'^{[3(\alpha-1)]}$. As yet there is no corresponding asymptotic theory for the eigenvalues at general values of ϵ, but the points approach the vertical axis along a straight line, as expected. The limiting values of $\epsilon\lambda_n$ as $\epsilon \to 0$, according to the asymptotic analysis of LHD, were shown in figure 2 above. It will be seen that these are in reasonable agreement with the present calculations.

Figure 8 (*a–d*) shows the profiles of the lowest unstable mode ($n = 1$) for $q/c = 0.25$, 0.20, 0.10 and 0.02. The dashed line in each figure shows the profile of the unperturbed solitary wave for the corresponding value of q/c. The horizontal axis is the original horizontal coordinate x for which $g = 1$ and $d = 1$. It can be seen clearly that the length scale of the normal mode gradually diminishes as $q/c \to 0$ and the perturbation is confined to a narrower region around the crest in a similar manner as that we observed for the first unstable mode of the deep-water wave (see figure 3). When we replot in figure 9 those profiles as functions of the scaled coordinate x/l (that is x/ϵ'^2 in our scaling), there appears to be a convergence of the profile for sufficiently small values of q/c (but see §6 below). Figure 10 compares the profile of the first unstable mode when $q/c = 0.25$ (solid line) with the profile of the trivial neutral mode corresponding to a horizontal shift (dashed line); this is simply the derivative of the profile of the steady solitary wave, for this value of q/c. According to Saffman (1985) the trivial neutral mode and the non-trivial mode should become identical at the point where the non-trivial mode exchanges its stability. As the critical point for the lowest non-trivial mode, which is equal to the first maximum of the total energy, is $q/c \approx 0.259$ as figure 6 indicates, the case shown in figure 10 ($q/c = 0.25$) is supercritical (in this sense) only marginally. The closeness of the two profiles shown in figure 10 can be regarded as an indication that our numerical results are in accord with Saffman's theory.

Figure 11 (*a–d*) shows the profile η_2 of the second unstable mode as a function of x for $q/c = 0.05$, 0.04, 0.03 and 0.02, respectively. The first three curves are also plotted

https://doi.org/10.1017/S0022112096004028 Published online by Cambridge University Press

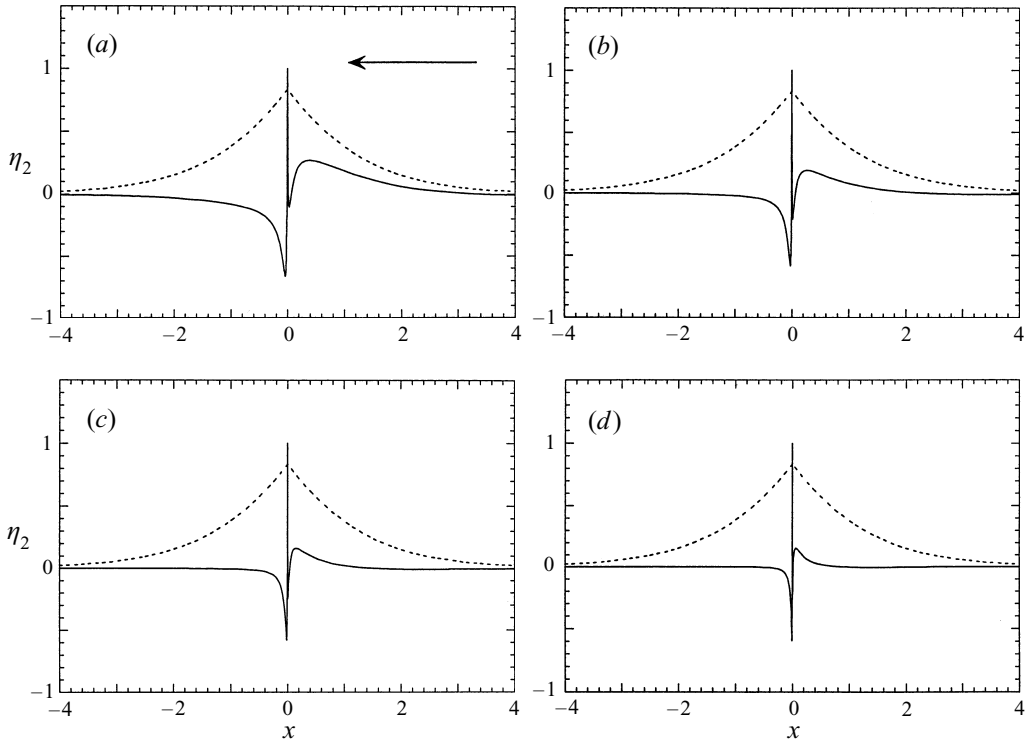


FIGURE 11. Profile of the second unstable mode of the solitary wave (solid line). The dashed curve shows the unperturbed wave profile: (*a*) $q/c = 0.25$, (*b*) $q/c = 0.20$, (*c*) $q/c = 0.10$, (*d*) $q/c = 0.02$.

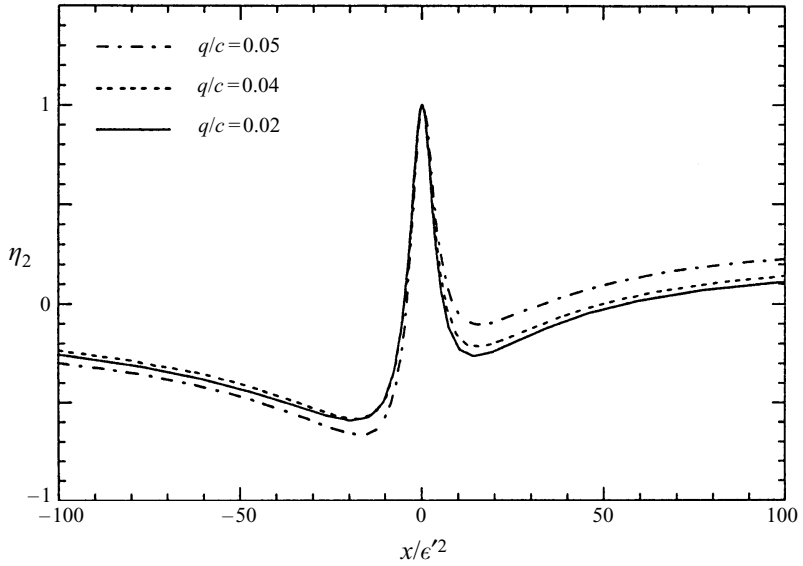


FIGURE 12. Profiles of the second unstable mode of the solitary wave plotted against the scaled coordinate x/ϵ'^2.

https://doi.org/10.1017/S0022112096004028 Published online by Cambridge University Press

as functions of x/l in figure 12. The profile for $q/c = 0.02$ is practically indistinguishable from the profile for $q/c = 0.03$.

6. Comparison of the deep-water wave and solitary wave

For general values of the deep-water wave steepness ak or the solitary wave steepness H/d the rates of growth of the instabilities are not directly comparable as functions of ϵ, since the parameters ϵ and ϵ' depend on external parameters and hence are defined differently in the two cases. However the inner length and time scales

$$l = \frac{q^2}{2g}, \quad \tau = \frac{q}{g} \tag{6.1}$$

depend only on the velocity q, for fixed g, and not on ϵ, so that the scaled frequencies

$$\lambda\tau = \frac{\lambda q}{g} \tag{6.2}$$

can be compared in the limit as $\epsilon \to 0$.

For the limiting deep-water wave we have from figure 13, since $q = \sqrt{2}\epsilon$,

$$\frac{\lambda_1 q}{g} = 0.0621, \quad \frac{\lambda_2 q}{g} = 0.016. \tag{6.3}$$

This can be compared with the limiting solitary wave for which, from figure 7,

$$\frac{\lambda_1 q}{g} = 0.0621, \quad \frac{\lambda_2 q}{g} = 0.014. \tag{6.4}$$

On the other hand the limiting values according to the asymptotic theory of the almost-highest wave (LHD) are

$$\frac{\lambda_1 q}{g} = 0.061(4), \quad \frac{\lambda_2 q}{g} = 0.01(8). \tag{6.5}$$

The above values are reasonably consistent, but the extrapolated eigenvalues in (6.3) and (6.4) are closer to each other than to those in (6.5), suggesting that the present calculations are more accurate.

For a similar reason we can legitimately compare the eigenfunctions only in the limit as $\epsilon \to 0$, by taking as a horizontal scale the length $l = q^2/2g$ which is independent of ϵ. In figure 14 is a comparison of the first unstable mode of the deep-water wave when $\omega = 0.84$ ($\epsilon = 0.1509$) with the corresponding mode of the solitary wave when $q/c = 0.16$ ($\epsilon' = 0.1279$), but neither of these is necessarily close to the limiting form. For, the agreement may be due partly to a similarity between the next-lowest-order corrections to the inner solutions in these two cases.

In figure 15 we compare the first mode of the solitary wave when $q/c = 0.02$ ($\epsilon' = 0.0183$) with the first unstable mode of the almost-highest wave (from LHD). The general similarity is clear, but there are significant differences. We remark that even at this value of ϵ some differences are still to be expected, because the eigenfunction for the almost-highest wave is that for the inner solution only, valid only when x is of order ϵ^2, i.e. $x/l = O(1)$. Even in this zone there are necessarily corrections of order $\epsilon^{3(\lambda-1)}$ (see LHD, §2). Further, in the matching zone where $x = O(\epsilon)$, i.e. $x/l = O(\epsilon^{-1})$, there are $O(1)$ corrections to the inner solution. Thus even for the solitary-wave instability shown in figure 15, when $\epsilon' = 0.0183$, there are $O(1)$ corrections to the inner solution

https://doi.org/10.1017/S0022112096004028 Published online by Cambridge University Press

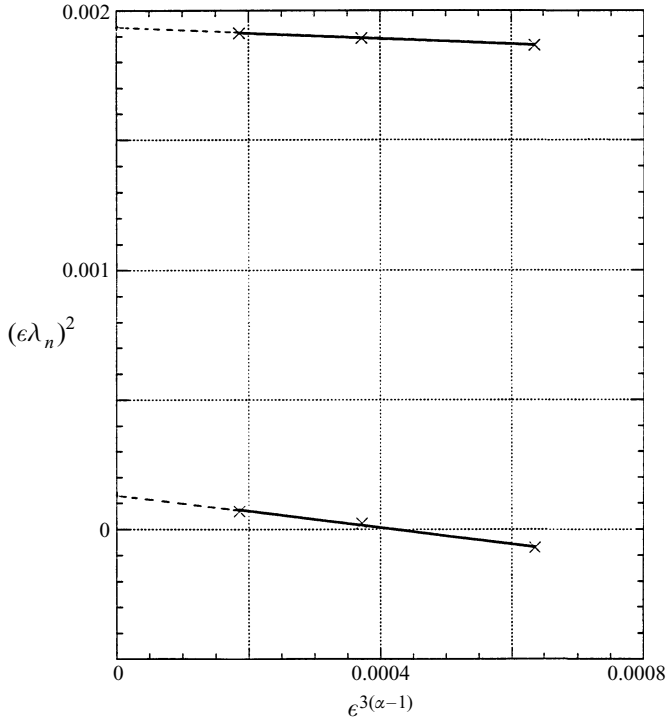


FIGURE 13. Extrapolation of the eigenfrequencies $\epsilon\lambda_1$ and $\epsilon\lambda_2$ for the deep-water wave, from the three lowest calculated values of ϵ. The fitted lines are given by $y = 0.0019305 - 0.10138\,x$ when $n = 1$ and by $y = 0.0013251 - 0.31477\,x$ when $n = 2$.

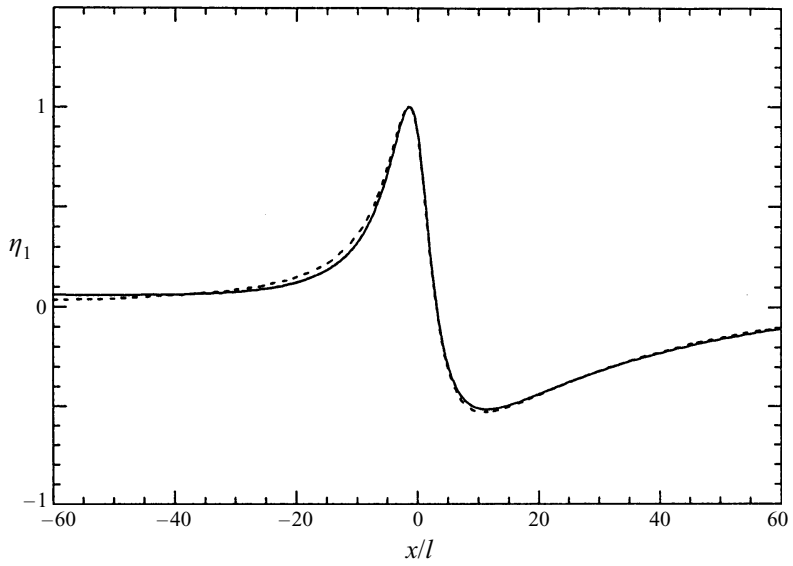


FIGURE 14. Comparison of the first unstable mode of a deep-water wave ($\omega = 0.84$, solid curve) with that of a solitary wave ($q/c = 0.16$, dashed curve).

https://doi.org/10.1017/S0022112096004028 Published online by Cambridge University Press

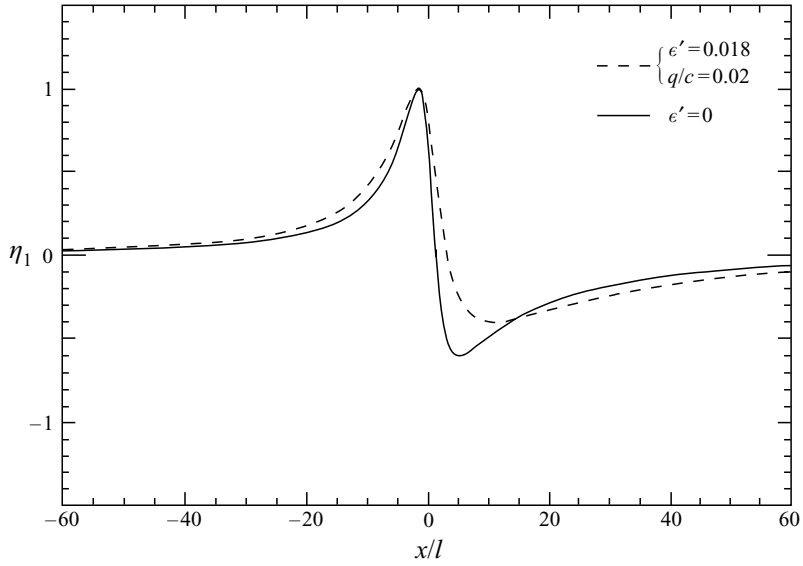


FIGURE 15. Comparison of the first unstable mode of a solitary wave ($q/c = 0.02$, dashed curve) with the lowest mode for the inner solution when $\epsilon = 0$ (LHD, solid curve).

when x/l is of order 50. However, when x/l is of order 5, say, we would expect closer agreement than is evident in the figure.

The eigenfunction for the solitary wave at $q/c = 0.02$ shown in figure 15 is very close to the solitary-wave eigenfunction at $q/c = 0.16$ shown in figure 14, which suggests that it has effectively converged, especially in the inner zone where x/l is of order 1. Probably, therefore, the present determination of the lowest mode is more accurate than that presented in LHD.

7. Conclusions and discussion

Our extended calculations of the lowest superharmonic instabilities of Stokes waves in deep water strongly support the conclusion that these are indeed 'crest instabilities', as first suggested by Longuet-Higgins & Cleaver (1994) and Longuet-Higgins *et al.* (1994); the numerical details being as revised by LHD.

Each crest instability first arises at a wave steepness ak corresponding to a stationary value of the energy density E. At that value of ak it has the form of a pure phase shift and so is not localized at the wave crest. However, our calculations have followed the development of the two lowest instabilities ($n = 1$ and 2) as the wave steepness ak approaches its limiting value. For the lowest mode ($n = 1$) the eigenfrequencies agree very closely with the asymptotic values given in LHD. The eigenfunctions also converge well and are in reasonable agreement with the lowest instability of the almost-highest wave as determinated by LHD.

Contrary to a conclusion stated in Longuet-Higgins & Cleaver (1994) and Longuet-Higgins *et al.* (1994), a second superharmonic instability ($n = 2$) has been found and its eigenfrequency is consistent with the results of LHD. There is no doubt that higher instabilities ($n > 2$) exist also.

Similar results have been obtained for solitary waves in shallow water, with increased accuracy. There again the scaling introduced by Longuet-Higgins & Cleaver (1994) and Longuet-Higgins *et al.* (1994) is found to govern the form and growth rates

https://doi.org/10.1017/S0022112096004028 Published online by Cambridge University Press

of the instabilities, as the solitary waves approach their maximum steepness. It should be emphasized that the present computations apply only to the linear stages of the crest instability. The nonlinear stages have been investigated by LHD and have been shown to lead in some cases to overturning and breaking of the wave crests; see also Tanaka *et al*. (1987) and Jillians (1989). In this study we have neglected the effects of surface tension, which may have a strong effect on the crest instability of any surface wave whose length is less than 2 m – perhaps more – for example through the production of parasitic capillary waves. Once such short-scale features occur, the influence of viscosity will increase drastically. These effects are presently under investigation by the authors.

We admit that our results can apply to wind waves in only a limited sense. For, whereas we have treated the instability of a uniform wave train, a typical ocean wave spectrum displays strong wave grouping and a wide range of length scales. Both of these features will be associated with other types of wave instability, and hence wave breaking. Nevertheless, the crest instabilities that we have considered here are essentially localized phenomena. Hence they may typify the final stages of breaking in other circumstances, provided the local scale is sufficiently great to avoid the effects of surface tension.

M.S.L.-H. gratefully acknowledges the support of the US Office of Naval Research under Contract N00014-91-J-1582.

REFERENCES

Cleaver, R. P. 1981 Instabilities of surface gravity waves. PhD thesis, University of Cambridge.

Jillians, W. J. 1989 The superharmonic instability of Stokes waves in deep water. *J. Fluid Mech.* **204**, 563–579.

Kharif, C. & Ramamonjiarisoa, A. 1990 On the stability of gravity waves on deep water. *J. Fluid Mech.* **218**, 163–170.

Longuet-Higgins, M. S. & Cleaver, R. P. 1994 Crest instabilities of gravity waves. Part 1. The almost-highest wave. *J. Fluid Mech.* **258**, 115–129.

Longuet-Higgins, M. S., Cleaver, R. P. & Fox, M. J. H. 1994 Crest instabilities of gravity waves. Part 2. Matching and asymptotic analysis. *J. Fluid Mech.* **259**, 333–344.

Longuet-Higgins, M. S. & Dommermuth, D. G. 1997 Crest instabilities of gravity waves. Part 3. Nonlinear development and breaking. *J. Fluid Mech.* **336**, 33–50 (referred to herein as LHD).

Longuet-Higgins, M. S. & Fox, M. J. H. 1977 Theory of the almost-highest wave: the inner solution. *J. Fluid Mech.* **80**, 721–741.

Longuet-Higgins, M. S. & Fox, M. J. H. 1978 Theory of the almost-highest wave. Part 2. Matching and analytic extension. *J. Fluid Mech.* **85**, 769–786.

Longuet-Higgins, M. S. & Fox, M. J. H. 1996 Asymptotic theory for the almost-highest solitary wave. *J. Fluid Mech.* **317**, 1–19.

MacKay, R. S. & Saffman, P. G. 1986 Stability of water waves. *Proc. R. Soc. Lond.* A **406**, 115–125.

Saffman, P. G. 1985 The superharmonic instability of finite-amplitude water waves. *J. Fluid Mech.* **159**, 169–174.

Tanaka, M. 1983 The stability of steep gravity waves. *J. Phys. Soc. Japan* **52**, 3047–3055.

Tanaka, M. 1986 The stability of solitary waves. *Phys. Fluids* **29**, 650–655.

Tanaka, M. 1995 On the "crest instabilities" of steep gravity waves. *Workshop on Mathematical Problems in the Theory of Nonlinear Water Waves, CIRM, Luminy, France, May 1995* (Abstract only).

Tanaka, M., Dold, J. W., Lewy, M. & Peregrine, D. H. 1987 Instability and breaking of a solitary wave. *J. Fluid Mech.* **185**, 235–248.

Zufiria, J. A. & Saffman, P. G. 1986 The superharmonic instability of finite-amplitude surface waves on water of finite depth. *Stud. Appl. Maths* **74**, 259–266.

https://doi.org/10.1017/S0022112096004028 Published online by Cambridge University Press